



Published in final edited form as:

Nat Neurosci. 2015 October ; 18(10): 1501–1508. doi:10.1038/nn.4110.

Basal forebrain neuronal inhibition enables rapid behavioral stopping

Jeffrey D. Mayse^{1,2}, Geoffrey M. Nelson², Irene Avila², Michela Gallagher¹, and Shih-Chieh Lin^{2,*}

¹Department of Psychological and Brain Sciences, Johns Hopkins University, Baltimore, MD, USA

²Neural Circuits and Cognition Unit, Laboratory of Behavioral Neuroscience, National Institute on Aging, National Institutes of Health, Baltimore, MD, USA

Abstract

Cognitive inhibitory control, the ability to rapidly suppress responses inappropriate for the context, is essential for flexible and adaptive behavior. While most studies on inhibitory control have focused on the fronto-basal-ganglia circuit, here we explore a novel hypothesis and show that rapid behavioral stopping is enabled by neuronal inhibition in the basal forebrain (BF). In rats performing the stop signal task, putative noncholinergic BF neurons with phasic bursting responses to the go signal were inhibited nearly completely by the stop signal. The onset of BF neuronal inhibition was tightly coupled with and temporally preceded the latency to stop, the stop signal reaction time. Artificial inhibition of BF activity in the absence of the stop signal was sufficient to reproduce rapid behavioral stopping. These results reveal a novel subcortical mechanism of rapid inhibitory control by the BF, which provides bidirectional control over the speed of response generation and inhibition.

Introduction

Inhibitory control is an essential aspect of executive function that allows humans and animals to rapidly suppress actions inappropriate for the behavioral context¹⁻⁵. An important paradigm to study inhibitory control is the stop signal task (SST), in which subjects must rapidly cancel a prepotent behavioral response when a go signal is occasionally followed by a stop signal^{6,7}. The SST is uniquely powerful in that it allows for the quantitative estimation of the latency to stop, the stop signal reaction time (SSRT)⁶. Understanding the neural mechanisms that determine SSRT is critical because SSRT is elevated in disorders

Users may view, print, copy, and download text and data-mine the content in such documents, for the purposes of academic research, subject always to the full Conditions of use:http://www.nature.com/authors/editorial_policies/license.html#terms

*Correspondence and requests for materials should be addressed to Shih-Chieh Lin (shih-chieh.lin@nih.gov).

Author Contributions

J.D.M., G.M.N. and S.L. designed the study. J.D.M., G.M.N. performed experiments and collected data. I.A. performed the electrical stimulation experiment. J.D.M., G.M.N. and S.L. analyzed data. J.D.M. and S.L. wrote the manuscript with inputs from G.M.N, I.A. and M.G.

Competing financial interests

The authors declare no competing financial interests.

characterized by deficient inhibitory control, including Parkinson's disease^{8,9} and attention-deficit hyperactivity disorder¹⁰, as well as in normal cognitive aging¹¹⁻¹³.

The fronto-basal-ganglia circuit has been widely implicated as the candidate neural circuit mechanism underlying rapid inhibitory control^{3-5,14-18}. Neuronal recordings in this circuit have identified movement initiation and other control signals in motor cortical regions that are differentially recruited depending on whether stopping is successful or not^{3,4}. A recent study further identified an early gating mechanism in the substantia nigra pars reticulata (SNr) that transiently pauses the planned action well in advance of SSRT¹⁸. Despite these advances, it remains unknown whether rapid behavioral stopping also requires mechanisms outside of the fronto-basal-ganglia circuit.

In this study, we explored a novel hypothesis outside of the fronto-basal-ganglia circuit and investigated the role of the basal forebrain (BF) in inhibitory control. The BF is one of the largest neuromodulatory systems, comprised of mainly magnocellular cholinergic and GABAergic cortically-projecting neurons^{19,20}. The current study focused on a physiologically homogeneous group of putative noncholinergic BF neurons that respond to motivationally salient stimuli with robust bursting responses²¹⁻²³. Because BF activity is tightly coupled with the speed of initiating behavioral responses, measured by reaction time (RT)²⁴, we investigated whether BF neuronal activity is also coupled with the speed of stopping, measured by SSRT⁷. Previous studies pointed to two opposing predictions about the potential role of BF neurons in rapid inhibitory control: one possibility is that BF neurons may show strong bursting responses to the motivationally salient stop signal²² to facilitate stopping. Alternatively, since stronger BF bursting is coupled with faster RT²⁴, arresting the preparation of the planned response may require inhibition of BF activity.

We tested these opposing predictions and found that, irrespective of whether successful stopping was rewarded, BF neurons that showed bursting responses to the go signal were inhibited nearly completely by the stop signal. The latency of BF neuronal inhibition was coupled with, and slightly temporally preceded, SSRT. Furthermore, artificially inducing BF inhibition caused stopping in the absence of the stop signal. These results identify a novel neural mechanism of SSRT in the BF that is outside of the fronto-basal-ganglia circuit.

Results

Rapid behavioral stopping in two variants of SST

To study the neural mechanism of inhibitory control, we have recently adopted the primate SST and developed a rodent-appropriate SST⁷. In the SST, rats are required to rapidly generate a behavioral response following an imperative go signal (sound), and to cancel the preparation of this response following an infrequent stop signal (light). Successful performance in stop trials requires rats to cancel the planned go response and maintain fixation for an additional 500ms wait period to receive reward (Stop Reward Task, Fig. 1a). By comparing the timing of fixation port exit in go and stop trials, we found that rats rapidly inhibited their prepotent go responses in stop trials, and that SSRT can be estimated without bias⁷ (Fig. 1b). As a result, stop trials can be partitioned into failure-to-stop trials and successful stop trials based on whether go responses were initiated before or after SSRT.

Successful stop trials can be further partitioned into failure-to-wait trials (not rewarded) and successful wait trials (rewarded)⁷ (Fig. 1b).

While the SST is a powerful task for studying inhibitory control, it is difficult to dissociate stop-related neuronal activity from reward-related neuronal activity using this task alone because successful stopping commonly leads to, and is therefore closely associated with, reward delivery. To resolve this ambiguity, and to dissociate stop- from reward-related neuronal activity, we developed a variant of SST in which stopping is not rewarded (Stop No Reward Task, Fig. 1c). This task was identical to the Stop Reward task except that animals do not receive reward in stop trials regardless of whether stopping was successful. While rats were not rewarded for stopping in the Stop No Reward Task, they nonetheless showed rapid behavioral stopping to the stop signal (Fig. 1d) with similar SSRTs as in the Stop Reward Task (Fig. 1e, independent samples t-test, $p=0.62$). In contrast, behavioral responses subsequent to SSRT were different in the two tasks when stopping was successful: rats stayed in the fixation port significantly longer and more frequently attempted to collect reward in the Stop Reward Task than in the Stop No Reward Task (Supplementary Fig. 1). The similarities and differences between the two SST variants allowed us to dissociate stop-related neuronal activity from reward-related neuronal activity. Specifically, we predict that the neural correlate of stopping should be common to both SST variants at epochs leading up to SSRT, while neural signals related to reward expectancy that develop after successful stopping should be present only in the Stop Reward Task within successful stop trials at epochs after SSRT.

BF neurons show opposite responses to go and stop signals

We recorded 494 well-isolated BF single units in 8 rats across 37 sessions while animals performed one of the two SST variants (4 rats each, Supplementary Fig. 2). The majority of recorded BF neurons (275/494) showed a rapid phasic excitatory response to the go signal (Fig. 2a) with baseline firing rates less than 12 spikes/s (mean \pm s.e.m., 3.45 ± 0.13 spikes/s). Bursting neurons were similarly found in the Stop Reward Task (161/235) and the Stop No Reward Task (114/259) (Supplementary Fig. 3). These BF bursting neurons share the same physiological properties with salience-encoding noncholinergic BF neurons described in previous studies²²⁻²⁶ and are the focus of subsequent analyses.

We first examined how BF neurons with bursting responses to the go signal respond to the stop signal. By comparing BF neuronal responses in stop trials to the activity of the same neurons in go trials at matching delays, we found that the stop signal did not elicit any additional excitatory response in BF neurons at the population level (Fig. 2b). Instead, these BF neurons were rapidly and nearly completely inhibited by the stop signal (Fig. 2b) in both SST variants (Supplementary Fig. 3). The stop signal led to significant inhibition in 92% (253/275) of BF bursting neurons (Fig. 2b-d, see online Methods). These neurons also constituted 83% (150/180) of BF neurons that were strongly inhibited by the stop signal with a decrease of at least 4 spikes/s (Fig. 2d). These results support that the go and the stop signal induced opposite responses – bursting and complete inhibition, respectively – in the same BF neuronal population, irrespective of whether successful stopping was rewarded.

BF neuronal inhibition is coupled with and precedes SSRT

Given that the amplitude of BF bursting response is correlated with RT²⁴, we next investigated whether the onset of BF neuronal inhibition is coupled with SSRT. In most BF bursting neurons, like the example in Fig. 3a, the onset of rapid and near complete neuronal inhibition was tightly coupled with SSRT. Eighty-eight percent of BF bursting neurons (243/275) had an onset of neuronal inhibition within 100ms of the estimated SSRT in that session that was, on average, -4.4 ± 1.8 ms earlier than SSRT (mean \pm s.e.m., $p=0.018$, paired t-test, Fig. 3b, 3c). On the population level, the onset of inhibition in BF bursting neurons preceded SSRT by at least 10ms (Fig. 3b). Additionally, between-session variabilities in BF inhibition latency for both individual neurons and for each session as a whole were significantly correlated with and slightly preceded SSRT across both SST variants (Pearson's correlation, Fig. 3d). Together, these data show that BF neuronal inhibition was coupled with and occurred slightly before SSRT. This observation suggests that BF neuronal inhibition provides a novel neural correlate of SSRT outside of the commonly studied fronto-basal-ganglia circuit.

Strongly bursting BF neurons are inhibited earlier

While the BF neuronal population was inhibited, on average, before SSRT, there was substantial variability in the inhibition latency of individual BF bursting neurons. We further investigated whether there were systematic differences between BF neurons that were inhibited earlier versus later relative to SSRT. We found that, in both SST variants, BF neurons that were inhibited earlier relative to SSRT showed stronger bursting responses to the go signal (Fig. 4a) and showed stronger inhibition by the stop signal in the peri-SSRT window (Fig. 4b). Consistent with these correlations, strongly bursting BF neurons (Fig. 4c) were strongly inhibited by the stop signal and were inhibited with earlier onsets that consistently preceded SSRT (Fig. 4d). These results therefore reveal systemic differences in BF neurons inhibited earlier versus later relative to SSRT, and suggest that BF neurons that were inhibited earlier than SSRT likely had stronger influences on behavior because they exhibited stronger bursting and stronger inhibition. The fact that strong BF inhibition reliably occurred before SSRT provides strong evidence that BF inhibition precedes, instead of follows, SSRT.

BF neurons are inhibited in both FS and SS trials

We next investigated whether BF neuronal inhibition was recruited differently in failure-to-stop and successful stop trials, as has been observed in the fronto-basal-ganglia circuit^{3,4,18}. In both SST variants, significant neuronal inhibition began around SSRT not only when stopping was successful (Fig. 5a,b, right panels), but also when stopping was not successful (Fig. 5a,b, left panels). Furthermore, strong BF neuronal inhibition from strongly bursting BF bursting neurons consistently preceded SSRT in both variants of SST regardless of whether stopping was successful (Fig. 5c, 5d). These observations suggest that the small differences in the relative timing between BF inhibition and SSRT in different trial types (Fig. 5a, 5b) likely resulted from differences in sampling of BF neurons in the two variants of SST, while the underlying temporal relationship between BF neuronal inhibition and SSRT remained the same in all trial types.

These observations indicate that, unlike the fronto-basal-ganglia circuit, the success or failure of stopping is not associated with differential engagement of BF neuronal inhibition. Instead, successful stopping is likely governed by the relative timing between go response initiation and BF neuronal inhibition. In other words, go responses are either initiated when they precede BF inhibition, or canceled when preceded by BF inhibition. These results support that BF inhibition represents a robust and invariant process engaged by the stop signal regardless of whether stopping is successful.

BF inhibition in FS trials reverses fixation exit at SSRT

Given the close association between BF neuronal inhibition and rapid behavioral stopping, we further investigated whether the presence of near-complete BF inhibition in failure-to-stop trials had any behavioral consequence. We found that, in failure-to-stop trials, rats frequently engaged in rapid reversal of their fixation port exit behavior (i.e. reentry), especially when they exited the fixation port right before SSRT (Fig. 6a, 6b, Supplementary Fig. 4). The timing of the fixation port exit and reentry were centered on SSRT (Fig. 6b), suggesting a delayed engagement of behavioral reversal in failure-to-stop trials outside of the fixation port that took place at SSRT. In support of this idea, analysis of accelerometer signals in failure-to-stop trials showed that, while outside of the fixation port, rats began to reverse their head withdrawal motion right around SSRT (Fig. 6c, 6d). These results suggest that, while BF neuronal inhibition did not occur in time to cancel the go response in failure-to-stop trials, BF neuronal inhibition still had a significant impact on behavior even after go responses have been initiated, leading to the late reversal of go responses starting at SSRT.

Post-SSRT BF neuronal activity tracks reward expectancy

In contrast to the highly similar onset of BF inhibition at SSRT in both failure-to-stop and successful stop trials (Fig. 5a, 5b), BF activity in both trial types diverged subsequent to SSRT (Fig. 7). In the Stop Reward Task, post-SSRT BF activity remained completely inhibited in failure-to-stop trials but was significantly higher in both types of successful stop trials (failure-to-wait and successful wait trials) (Fig. 7a). Furthermore, the post-SSRT ramping activity in failure-to-wait trials was significantly greater than in successful wait trials (Fig. 7a). Activity in failure-to-wait trials peaked right before the premature fixation port exit, and immediately began to decrease after fixation port exit (Fig. 7b). On the other hand, in the Stop No Reward Task, post-SSRT BF activity was similarly inhibited between failure-to-stop and successful stop trials where both trial types were not rewarded (Fig. 7c). Taken together, post-SSRT BF activity remained inhibited in all cases when reward was not expected, and only began to rebound when reward was expected in successful stop trials in the Stop Reward Task. These results support the interpretation that post-SSRT BF activity tracks the rising expectation of reward during the waiting period, which potentially led rats to exit prematurely in failure-to-wait trials. These results also highlight the importance in distinguishing neural activity associated with the fast behavioral stopping occurring at SSRT from the post-SSRT neural activity that reflects dynamic reward expectation.

Induced BF inhibition reproduces behavioral stopping

Finally, we tested whether BF inhibition plays a causal role in behavioral stopping (Fig. 8a). We utilized brief electrical microstimulation of the BF to inhibit BF bursting neurons based

on the observation that a short pulse of BF electrical stimulation inhibited BF bursting neurons for up to 1s after a brief rebound excitation (Fig. 8b, 8c). The long-lasting inhibition induced by electrical microstimulation was selective for BF bursting neurons and not observed in other BF neurons (Fig. 8b, Supplementary Fig. 5). We therefore tested whether artificially inducing BF inhibition in place of the visible stop signal may lead to behavioral stopping in rats that had never been trained in the SST (Fig. 8a). We found that the brief BF electrical stimulation was able to replace the stop signal and induced rapid behavioral stopping in 18/20 sessions (7 rats) (Fig 8c, 8d). In sessions with simultaneous BF recording and microstimulation, the onset of BF neuronal inhibition was closely associated with estimated SSRT (Fig 8c). Furthermore, animals often attempted to reenter the fixation port in failure-to-stop trials (Fig. 8c, 8e), similar to the reentry behavior observed in the SST (Fig. 6a, 6b, Supplementary Fig. 4). Reentry occurred despite the absence of an overt stop signal, and despite the fact that neither stopping nor reentry carried any behavioral consequence. Furthermore, the effect of BF stimulation on behavioral stopping did not result from rats perceiving the stimulation as an extra sensory cue (Supplementary Fig. 5). Together, these results support that BF neuronal inhibition plays a causal role in rapid inhibitory control.

Discussion

In this study, we examined the role of the basal forebrain (BF) in inhibitory control while rats performed two variants of the stop signal task (SST) (Fig. 1). We found that, irrespective of whether or not successful stopping was rewarded, BF neurons with bursting responses to the go signal were inhibited nearly completely by the stop signal (Fig. 2). The onset of BF inhibition was tightly coupled with and slightly preceded the latency of behavioral inhibition, the stop signal reaction time (SSRT) (Fig. 3, 4). Further, BF inhibition was similarly present in failure-to-stop trials (Fig. 5), and was coupled with the behavioral reversal of go responses at SSRT (Fig. 6). While BF neuronal inhibition was present in both SST variants, only in the Stop Reward Task did BF inhibition quickly rebound during the waiting period in successful stop trials, which closely tracked whether animals successfully waited and expected to receive reward (Fig. 7). Finally, artificially inducing BF inhibition via brief electrical microstimulation reproduced the full behavioral stopping phenotype in the absence of an overt stop signal (Fig. 8). Taken together, these results identify a novel neural correlate of SSRT in the BF and support that BF neuronal inhibition plays a causal role in enabling rapid inhibitory control. This novel BF inhibitory control mechanism takes place outside of the commonly studied fronto-basal-ganglia circuit^{3-5,14-18}.

SST performance is commonly conceptualized as a race between go- and stop-processes⁶. According to the race model, a neural signal that controls movement initiation, such as those in the fronto-basal-ganglia circuit^{3,4,18}, must differentiate its activity between successful and failed stopping, and must do so before SSRT³. Our results extend this theoretical framework and further suggest that, in the SST, the brain not only encodes movement initiation that reflects the outcome of the race, but also separately encodes the stopping process itself. A neuron that encodes the stop process itself should respond similarly to the stop signal regardless of whether or not stopping is successful, because such a neuron is a participant in the race and therefore agnostic to its outcome. We propose that BF inhibition represents just

such a neuronal stop process: a rapid and automatic inhibitory control process triggered by the stop signal that takes place in both variants of the SST irrespective of whether successful stopping was rewarded, and in both failure-to-stop and successful stop trials regardless of whether stopping was successful. The stop process embodied by BF inhibition therefore represents one component process of the race, the presence of which enables rapid behavior stopping, but is not sufficient to ensure successful stopping.

The idea that the brain encodes the stop process regardless of whether stopping is successful has important implications for identifying neural mechanisms of stopping because the success or failure of stopping is determined not by the recruitment of the invariable stop process, but by the relative timing between the invariable stop process and the variable process governing go response initiation. As a result, comparing neural activity between successful- and failure-to-stop trials will not identify neural correlates of the invariant stop process, such as BF inhibition. Rather, this comparison will like identify neural correlates associated with the variability of the go process (go-fast vs. go-slow), as well as neural correlates of post-SSRT evaluative signals, such as SEF activity²⁷ and the post-SSRT BF activity buildup. The experimental design was able to dissociate neuronal signals related to stopping (BF inhibition) from neuronal signals related to reward processing and anticipation (post-SSRT BF activity buildup in successful stop trials in the Stop Reward Task) by comparing BF activity in the two SST variants.

It is important to note that the stop process embodied by BF inhibition did not lead to freezing, because rats were able to exit or reenter the fixation port under complete BF inhibition in both SST variants (Fig. 3a, Fig. 6) as well as during stimulation-induced BF inhibition (Fig. 8c). This suggests that the effects of BF inhibition are specific to the prepotent response associated with the preceding go signal and do not produce global or general motor suppression. Our results further show that the BF stop process has a significant influence on behavior even when it was too late to cancel the initial go response in failure-to-stop trials, in which case BF inhibition was coupled with the late reversal of go responses starting at SSRT that oftentimes led to corrective reentry behaviors (Fig. 6 and Supplementary Fig. 4).

The current results significantly extend previous observations that highlight the functional significance of this group of putative noncholinergic BF neurons²²⁻²⁶. While previous studies strongly suggest that the activity of these BF neurons must be modulated in the SST, they offer conflicting predictions as to whether BF neurons should increase²² or decrease²⁴ firing rates in response to the stop signal. Our results here show that BF neurons responds to motivationally salient go and stop signals in opposite directions with bursting responses and inhibition, respectively, instead of displaying similar bursting responses to all motivationally salient stimuli²². This result challenges the simple view that BF neurons encode motivational salience at all times, and suggests that the lack of BF bursting responses toward the motivationally salient stop signal may reflect a context-dependent omission of bursting responses in the presence of a preceding predictive cue, similar to what has been observed in midbrain dopaminergic neurons^{28,29}. The current study also demonstrates that a stimulus can elicit BF inhibition without generating a preceding phasic bursting response, and supports that BF bursting and inhibition can be controlled independently of each other.

The central finding of the current study – the coupling between BF inhibition and SSRT – is novel and cannot be predicted by previous studies of BF neurons. On the one hand, while the coupling between BF inhibition and the cancelation of the go response in Nogo trials has been previously suggested using the Go/Nogo task²², the Go/Nogo task cannot provide estimates of SSRT and therefore cannot predict whether and how BF inhibition will be coupled with SSRT in the current study. On the other hand, while the overall direction of BF activity modulation in the SST is consistent with the coupling between BF bursting strengths and faster RTs²⁴, the ways in which BF bursting and BF inhibition are coupled with RT and SSRT, respectively, are very different. Specifically, while BF bursting was time-locked to stimulus onset but not to RT, the current study found that BF inhibition was tightly coupled with SSRT but not to stop signal onset.

The causal role of BF inhibition in enabling rapid stopping is supported by the BF electrical stimulation experiment. While electrical stimulation is a non-selective method that can activate many types of local neurons, brief stimulation of the BF appears to produce a specific effect – rebound excitation followed by sustained inhibition – on BF bursting neurons (Fig.8, Supplementary Fig. 5). Similar compound excitation-inhibition effects of electrical stimulation have been reported in cortical circuits³⁰⁻³². If the stimulation-induced rebound BF excitation were to impact behavior, one would predict to see speeding of RTs, because BF stimulation designed to enhance BF bursting amplitude leads to faster RTs²⁴. Instead, in the current study, BF stimulation leads to rapid stopping, suggesting that the impact of the rebound excitation on behavior is either negligible or is overridden by the subsequent inhibition. Together with our previous BF stimulation experiment that leads to faster RTs²⁴, these two BF stimulation experiments suggest that the influence of BF stimulation on behavioral response is not mediated by the perception of BF stimulation as an additional internal or external sensory cue. Instead, BF's influence on behavior is dictated by the timing and duration of the same stimulation, such that the same stimulation can have bidirectional effects on RT on different trials (Fig S9 in Avila & Lin²⁴). The stimulation experiments support the conclusion that BF plays a role in modulating behavioral response bidirectionally.

Finally, our results support that rapid behavioral stopping is jointly controlled by the fronto-basal-ganglia circuit^{3-5,14-18} and by BF neuronal inhibition that serve complimentary roles. Neuronal activities in the basal ganglia, but not in the BF, have been shown to encode the variability of the go process (go-fast vs. go-slow)^{18,33,34}, provide an early gating mechanism^{18,35}, as well as encode specific motor responses^{18,33,34,36}. On the other hand, neuronal activity in the BF, but not in the basal ganglia, is tightly coupled with and also temporally precedes SSRT. Based on these observations, we suggest that the cortico-basal-ganglia loop is primarily in charge of selecting and executing a motor response (go), while noncholinergic BF neurons serve as a bidirectional gain modulation mechanism that either speeds up or cancels the selected motor response, respectively, via their bursting response²⁴ and neuronal inhibition. In our proposed model, the success of stopping is determined by the relative timing between the go process encoded by accumulating cortico-basal-ganglia activity and the stop process encoded by BF inhibition (Supplementary Fig. 6). The rapid modulation of behavioral execution by BF activity is likely mediated through its fast modulation of frontal cortical activity²⁶.

Online Methods

Subjects

Male Long-Evans rats (Charles River, NC), weighing 250-350g (3-5 months old) at the start of the experiment, were used in this study. Nineteen rats were trained in the Stop Reward Task, four of which subsequently underwent surgery to record BF neuronal activity. A separate group of eight rats were trained in the Stop No Reward Task, four of which underwent surgery to record BF neuronal activity. Another group of seven rats were trained to associate the go sound with reward only, and were subsequently used in BF electrical stimulation experiments.

Animals were housed individually in a temperature- and humidity-controlled vivarium on a 12L:12D cycle. Animals in the Stop Reward condition were provided *ad libitum* access to water and food-restricted to 85% of their free-feeding weight. Animals in the Stop No Reward condition and stimulation experiments were provided *ad libitum* access to food and water-restricted with body weight maintained at least 90% of their free-feeding weight. The water-restricted animals received free access to water for fifteen minutes at the end of each day and were provided 48 hours free access to water weekly.

All experimental procedures were conducted in accordance with the National Institutes of Health (NIH) Guide for the Care and Use of Laboratory Animals and approved by the National Institute on Aging Animal Care and Use Committee.

Apparatus

Behavioral training and neurophysiological recording were conducted in custom-built behavioral chambers by Med Associates Inc. (St. Albans, VT), described in detail previously⁷. Briefly, each chamber was equipped with one photo-beam lickometer reward port (CT-ENV-251L-P) located in the center of the front panel. Diluted liquid sweetened condensed milk (2:1 water:milk) or water was used as reward and delivered through a custom-built multi-barrel sipper tube. Reward delivery was controlled by the opening of a solenoid that was calibrated to deliver 10 μ l of fluid per opening (10ms). The reward port was flanked by two nosepoke ports (ENV-114M) that were each equipped with one IR sensor to detect port entry and exit. Only the right nosepoke port was used in behavioral training as the fixation port. Behavior training protocols were controlled by Med-PC software (Version IV), which stored all event timestamps at 2ms resolution. All behavioral sessions were recorded via overhead video cameras and data were stored offline for later analysis.

Stop Signal Task

Detailed behavioral shaping and training procedures for the Stop Reward Task have been described in detail previously⁷. Briefly, all rats were first shaped to enter the right fixation port. After a variable foreperiod, selected pseudorandomly from [0.35, 0.5, 0.65, 0.8]s, a 6kHz tone (80dB, 2s) was presented, signaling reward availability. If rats began licking within 3s of tone onset, they received 30 μ l of reward starting at the third lick. The inter-trial interval (ITI) was 1-3 sec and was not signaled to the rat. Either premature fixation port

entry or premature licking during ITI both reset the ITI timer. Animals were held at this stage for 10-14 sessions to encourage fast responding to the tone before they underwent additional training.

After the initial behavioral shaping, rats in the BF electrical stimulation experiment did not receive any additional training (Fig. 8a). Rats in the Stop No Reward task were transitioned to the full Stop No Reward contingency without any intermediate training. In this task, a stop signal (white central panel light, 0.5s) was presented in one-third of trials after a variable stop signal delay (SSD). Rats were not rewarded on those stop trials (Fig. 1c). The five SSDs were determined before the start of each session based on animals' performance in the previous session, and the SSD was chosen pseudorandomly from these five SSDs on each trial. Every session included a 0ms SSD such that the tone and light were presented simultaneously. The remaining four SSDs were evenly spaced in 40ms steps and adjusted by experimenters between sessions to ensure approximately 50% failed stop trials.

Rats in the Stop Reward condition underwent additional shaping to associate a light signal with reward if they responded after, but not before, light offset. The overall organization of the task was the same as the previous shaping phase, except that the 6kHz tone was replaced by illumination of a white central panel light in each trial. This light would subsequently serve as the stop signal in the SST. Fixation port exit responses during light illumination led to forfeiture of reward, and only responses that occurred after light offset led to 30 μ l of reward. The duration of light illumination was adaptively increased until animals could reliably wait for 500ms (10-14 sessions). Rats were provided with explicit feedback for successfully waiting for the entire light duration in the form of an audible solenoid click similar to the click associated with reward delivery. After this training phase, rats received several refresher tone-alone sessions before transitioning to the Stop Reward Task.

In the Stop Reward Task, the 6kHz tone (go signal) was presented on all trials, and on 1/3 of the trials the go signal was followed by the light stop signal after a variable stop signal delay (SSD) (Fig. 1a). In tone-alone trials (2/3), or go trials, animals were required to make fast go responses ($RT < 500ms$) to receive reward. In the stop trials (1/3), reward was available only if wait time (WT), the latency between stop signal onset to fixation port exit, was longer than the 500ms hold duration (equivalent to $RT > SSD + 500ms$). The same amount of reward (30 μ l) was delivered in both fast go trials and successful stop trials. SSDs were determined similarly as in the Stop No Reward Task.

Subjects were trained in one daily session (60-90 minutes) and underwent stereotaxic surgery for implantation of chronic recording electrodes after reaching behavioral asymptote. Following 7-14 days of recovery, animals were again food- or water-restricted and behavioral training resumed.

Stereotaxic Surgery and Electrode

The stereotaxic surgery procedures were similar to those reported previously^{24,26}. After reaching behavioral asymptote, rats were removed from food or water restriction for 3d before undergoing stereotaxic surgery. Rats were anesthetized with isoflurane (3-5% induction followed by 1-3% maintenance), placed in a stereotaxic frame (David Kopf

Instrument, CA) that was fitted with atraumatic ear bars and a heating pad to maintain body temperature at 37° C. Multiple skull screws were inserted first, with one screw over the cerebellum that served as the common electrical reference, and a separate screw over the opposite cerebellum hemisphere that served as the ground. A custom-built 32-wire multi-electrode moveable bundle was implanted into bilateral BF. The electrode consisted of two moveable bundles each ensheathed in a 28-gauge stainless steel cannula. Each bundle contained 16 polyimide-insulated tungsten wires (38 µm diameter) (California Fine Wire, CA), with impedance ranging from 0.1-0.3 MΩ at 1kHz (niPOD, NeuroNexusTech, MI). The two cannulae of the electrode were precisely positioned to target the BF on both hemispheres at AP -0.6 mm, ML ±2.25 mm relative to Bregma³⁷. The cannulae were lowered to DV 6–6.3 mm below cortical surface using a micropositioner (Model 2662, David Kopf Instrument), and the electrodes were advanced to 7 mm below the cortical surface. After reaching target depth, the electrode and screws were covered with dental cement (Hygenic Denture Resin). Rats received acetaminophen (300 mg/kg, aq. oral delivery) post-surgery and allowed 7-14 days to recover. Cannulae and electrode tip locations were verified with cresyl violet staining of histological sections at the end of the experiment and were compared with reference anatomical planes³⁷ (Supplementary Fig. 2).

Recording

Each recording session lasted 60-90 minutes. Several recording sessions were collected at each electrode depth (separated by 125 µm), and a single session was included in data analysis based on the quality of behavioral and physiological data. Therefore, each recording session represents a distinct sample of BF single neuron ensembles. Electrical signals were referenced to a common skull screw placed over the cerebellum, filtered (0.03 Hz-7.5 kHz), amplified using Cereplex M digital headstages, and recorded using a Neural Signal Processor (Blackrock Microsystems, UT). Single unit activity was further bandpass filtered (250 Hz-5 kHz) and recorded at 30 kHz. Spike waveforms were sorted offline using OfflineSorter V.3 (Plexon Inc, TX). Only single units with clear separation from the noise cluster and with minimal ($\leq 0.1\%$) spike collisions (spikes with less than 1.5ms interspike interval) were used for further analyses. Additional cross-correlation analyses were used to remove duplicate units recorded simultaneously over multiple electrodes. Only neurons with at least 0.1Hz baseline firing rates were included in the analysis. A total of 494 well-isolated BF single units were recorded from 37 sessions across 8 rats in the SST (Stop Reward: 4 rats, 17 sessions, 235 neurons; Stop No Reward: 4 rats, 20 sessions, 259 neurons).

Estimation of SSRT using the modified integration method

SSRT was estimated using the modified integration method that we have previously developed and validated⁷. This novel method provides an estimate of SSRT by directly comparing RT distributions in stop trials and go trials in order to determine the time point at which the stop signal begins to slow down RTs relative to go trial RTs (Fig. 1b, 1d). Specifically, we randomly sampled n go trials (n = the number of stop trials in a session) and subtracted from the sampled go trial RTs the SSDs associated with stop trials. This procedure created a new RT distribution such that go trial RTs were re-aligned to would-be stop signals in order to compare with the stop trial cumulative RT distribution aligned to the onset of the stop signal. This sampling procedure was repeated 10,000 times to construct a

conservative 99.9% (0.05% - 99.95%) confidence interval (CI) of the cumulative re-aligned go trial RT distribution. We determined the earliest time point in the sorted stop trial cumulative RT distribution at which RTs began to significantly slow down relative to the 99.9% CI, representing a conservative upper bound of the SSRT estimate ($SSRT_{UpperBound}$). Failure-to-stop (FS) trials were defined as trials in which WT was less than $SSRT_{UpperBound}$. Successful stop (SS) trials had WTs longer than $SSRT_{UpperBound}$. In the Stop Reward Task, successful stop trials were further divided into failure-to-wait (FW) trials ($SSRT_{UpperBound} < WT < 500\text{ms}$; not rewarded) and successful wait (SW) trials ($WT > 500\text{ms}$; rewarded). Finally, to provide an unbiased estimate of the SSRT, we took the mean of the re-aligned cumulative go trial RT distributions, and determined the time point in this distribution that corresponded to the probability $p(\text{failure-to-stop})$ as the SSRT estimate. The resulting SSRT estimate was not affected by the number of stop trials in a session and the choice of confidence level, and provided an unbiased estimate, as was validated using simulated data⁷. This SSRT estimate method therefore provided the most sensitive yet accurate estimates of the true SSRT.

To establish the confidence interval of the SSRT estimates, we used the same simulation procedure described in Mayse et al⁷ where the true SSRT was known, and determined the 95% CI of the difference between the mean SSRT estimate and the true SSRT. Each of the 1000 simulation runs consisted of the same number of sessions used in the group estimate (Figures 3-7) ($n = 37, 17, 20$, respectively for all, only Stop Reward, or only Stop No Reward sessions), as well as the number of go and stop trials in those sessions. The 95% CIs were $[-5.8, 5.4]$ ms for all sessions, $[-8.3, 7.5]$ ms for Stop Reward sessions, and $[-7.8, 7.6]$ ms for Stop No Reward sessions, and were shown as red shaded areas around SSRT in these figures.

Identification of BF Bursting Neurons

Peri-stimulus time histograms (PSTHs) were generated for each BF single neuron against each behavioral event using 10ms bins. All PSTHs in figures were smoothed with a 3-point Hanning window for visualization purposes only. To determine whether BF neurons showed significant responses to the go signal, we compared PSTHs to the go signal (in go trials) with foreperiod-matched PSTHs during the nosepoke fixation period before go signal onset. This difference in firing rates between the two conditions (Fig. 2a) allowed us to control for fluctuations in firing rates associated with nosepoke fixation, and to identify true responses to the go signal as significant deviations in the difference PSTH from the zero baseline. The response amplitude to the go signal (Fig. 2c, 2d) was defined as the average firing rate of the difference PSTH at the $[0.05, 0.2]$ s window.

BF bursting neurons were identified based on two criteria: (1) the presence of a significant excitatory response in the $[0.01, 0.2]$ s window after go signal onset, and (2) baseline firing rates less than 12 spikes/s (Fig. 2c)²²⁻²⁶. The baseline firing rate was defined as the mean firing at $[-2, -1]$ s before onset of the go signal. The statistical significance of the difference PSTHs was determined by comparing cumulative frequency histograms (CFHs) of PSTHs after tone onsets against the cumulative sum distribution of baseline PSTHs before tone onset ($[-1.5, 0]$ s), estimated based on 1,000 bootstrapped samples ($p < 0.01$, two-sided)³⁸.

A minimum response amplitude of 0.05 spikes per response was required to be considered a significant response.

To determine whether the population PSTHs on go trials and foreperiod-matched control trials were significantly different, we used paired t-tests at each 10ms bin, with Bonferroni's correction for multiple comparisons (α/n , where $\alpha = 0.01$ and $n=40$ is the number of 10ms bins). The same method was used to compare population PSTHs in Figures 2b & 7, with statistical significance indicated by horizontal bars. BF bursting amplitude (Fig. 4a) was defined as the average firing rate to the go signal (in go trials only) in the [50,160]ms window.

BF Neuronal Responses to the Stop Signal

To determine whether BF neurons showed significant responses to the stop signal, it is important to control for neuronal responses to the go signal that preceded the stop signal by a variable SSD. For this purpose, we compared PSTHs to the stop signal against latency-matched go trial controls using a random permutation method (Fig. 2b). Specifically, we randomly sampled n go trials (n is the number of stop trials) and added to the timestamp of go signals the SSDs associated with the stop trials. We calculated PSTHs aligned to this new set of would-be stop signals that had the same SSDs relative to go signals. The random sampling procedure was repeated 10,000 times, and the mean of 10,000 PSTHs was taken as the PSTH for latency-matched go trial controls. Deviations of the difference PSTH (stop minus latency-matched controls) from the zero baseline indicate significant responses to the stop signal. By applying the method described earlier that used cumulative sums in the baseline period³⁸ ($p < 0.01$, two-sided), 253/275 BF bursting neurons showed significant inhibition to the stop signal. The response amplitude to the stop signal (Fig. 2d) was defined as the average firing rate of the difference PSTH at the [0.1, 0.5]s window. Similar procedures were employed to calculate BF responses relative to the estimated SSRT, which were implemented by first aligning PSTHs to the estimated SSRT within each session before averaging across sessions (e.g. Fig. 3b, 5a, 5b). The amplitude of peri-SSRT BF inhibition (Fig. 4b) was defined as the average firing rate reduction in all stop trials compared to latency-matched controls in the [-50,50] ms window around SSRT.

To determine how BF neurons respond to the stop signal in FS and SS trials, we modified the random permutation method and identified latency-matched go trial controls separately for FS and SS trials (Fig. 5a, 5b). Specifically, in each random sample of n go trials, we computed WT for each trial as the difference between its go trial RT and the randomly assigned SSD. Trials with WT less than $SSRT_{UpperBound}$ were used as latency-matched controls for FS trials, while trials with WT longer than $SSRT_{UpperBound}$ were used as controls for SS trials.

Estimating BF neuronal inhibition latency

To determine neuronal inhibition latency for individual BF bursting neurons (Fig.3b), we first identified all 10-ms bins in the SSRT-aligned PSTHs that were inhibited by more than 1 spk/s relative to control PSTHs generated from latency-matched go trials. BF neuronal inhibition onset was defined as the first 10-ms inhibited bin that led a 100-ms interval in

which 9/10 bins were inhibited by more than 1 spk/s. This method is highly specific in identifying the onset of strong inhibition and produced false alarm rates of $<4 \times 10^{-4}$ in the baseline periods ($[-0.5, -0.1]$ s relative to SSRT). Under this definition, eighty-eight percent of BF bursting neurons (243/275) had neuronal inhibition onset within $[-0.1, 0.1]$ s of the estimated SSRT within each session (Fig. 3b).

The same method was used to estimate inhibition latency for all BF bursting neurons relative to SSRT in a session (Fig. 3d) and for the entire population (Fig. 3b, 4d, 5). Specifically, we first pooled the activity of all BF bursting neurons recorded in a session or for the entire population as a multiunit, and estimated neuronal inhibition onset based on the activity of this multiunit. To include the contributions of weakly inhibited BF bursting neurons that didn't meet the stringent 1 spk/s inhibition threshold but were nevertheless inhibited around SSRT (Fig. 3b), we included all BF bursting neurons that had lower average activity in the $[-0.05, 0.05]$ s window around SSRT compared to latency-matched go trial controls ($n=260/275$). To ensure sufficient sampling of BF activity in individual session analysis, we only analyzed sessions with at least four such BF bursting neurons ($n=24/37$ sessions).

BF Neuronal Responses to fixation exit in FW and SW trials

Fixation port exits in FW and SW trials occurred under very different circumstances: in FW trials, rats exited the fixation port during the waiting period in the absence of an audible solenoid click. In contrast, in SW trials, rats exited the fixation port after hearing the audible solenoid click that signaled reward availability. Therefore, the responses time-locked to fixation exits in FW and SW trials cannot be compared with each other directly. Instead, we realigned SW trials to would-be fixation exits that were latency-matched to the WT in FW trials (Fig. 7c). This allowed us to compare the activity of FW and SW during the same epochs in the waiting period prior to fixation exit in FW trials.

Reentry behavior

Reentry behavior in stop trials (Fig. 6a, 6b) and in stimulation trials (Fig. 8e) was defined by two criteria: (1) the latency between fixation port exit and reentry must be less than 1s; and (2) rats must reenter the fixation port before entering the reward port. Comparison of reentry behavior in different tasks is further discussed in Supplementary Fig. 4.

Accelerometer signals

A three-axis accelerometer (ADXL327, Analog Devices) was attached to the Cereplex M digital headstage and signals were digitized at 1kHz and recorded simultaneously with neural signals. Accelerometer signals were recorded from 3 rats over 15 sessions (Stop Reward Task, 1 rat, 2 sessions; Stop No Reward Task, 2 rats, 13 sessions).

Since accelerometers also detect gravity, and the projection of gravity on the three axes changes depending on the orientation of the accelerometer at any given moment, accelerometer signals alone are not sufficient to reconstruct the speed and position of the animal. The influence of gravity also makes it difficult to interpret the sign and amplitude of accelerometer signals. As a result, we only compared accelerometer signals between failure-

to-stop trials and latency-matched go trial controls to identify when accelerometer signals began to diverge. Our goal was to test the specific prediction that rats began to reverse their fixation port exit behavior in failure-to-stop trials right around SSRT.

We used the same random permutation method to identify latency-matched go trials for failure-to-stop trials, and aligned accelerometer signals at SSRT (Fig. 6c). Accelerometer signals in failure-to-stop trials were significantly different from latency-matched controls if they exceeded the 0.2% [0.1, 99.9] confidence interval (5,000 permutations) (Fig. 6c, 6d).

Electrical Stimulation

Seven rats were tested in the BF electrical stimulation experiment (20 sessions) after initial behavioral shaping procedures and without any additional training. The behavioral task (Fig. 8a) had the same structure as the Stop No Reward Task, except that the visual stop signal was replaced by brief BF electrical stimulation. Individual stimulation pulses were biphasic charge-balanced pulses (0.1 ms each phase) delivered through a constant current stimulator (stimulus isolator A365R, World Precision Instruments, FL), driven by a Master-8-VP stimulator (A.M.P.I., Israel). Each stimulation train consisted of 1 or 3 pulses delivered at 100 Hz (10 ms interstimulus interval). The stimulation was delivered through all 32 electrodes in the BF, the same electrode configuration as used in the recording experiment. This was intended to mimic the widespread presence of BF bursting neurons throughout the recording region, representing an ensemble bursting event of the entire population^{24,26}. Stimulation current level was set at 24 - 48 μ A per electrode, which was based on the effective stimulation intensities used in earlier studies^{24,26}.

In a subset of sessions ($n=11$, 4 rats), BF electrical stimulation was delivered only through half of the electrodes (8/16) within each bundle (in each hemisphere), while single unit activity was recorded on the remaining wires to verify the effect of microstimulation on BF neuronal activity ($n = 44$ single units). These 44 single units were further classified into bursting ($n=21$) and non-bursting (other) neurons ($n=23$) based on their responses to the go signal (Fig. 8b). Recording artifact related to microstimulation was minimized by: (1) delivering stimulation current from one BF bundle and returning the current from another BF bundle in the contralateral hemisphere. This current return path minimized the interference with ground or reference electrodes on the skull used for recording; (2) temporarily increasing the lower bound of high-pass filter in the front end amplifier during the stimulation epoch using the fast-settle function in the Neural Signal Processor (Blackrock Microsystems). These steps allowed us to record single unit activity within 5ms of electrical stimulation.

Statistics

No statistical methods were used to pre-determine sample sizes but our sample sizes are similar to those generally employed in multi-electrode recording experiments with complex behavioral task designs in rodents. No randomization or blinding was used nor needed to assign rats to the only between subjects conditions, the Stop Reward and Stop No Reward tasks.

Statistical tests are individually described under appropriate sections in the methods. Non-parametric bootstrap methods require no specific assumptions of data distributions. In parametric tests, data distribution was assumed to be normal but this was not formally tested. A methods checklist is available with the supplementary materials.

Supplementary Material

Refer to Web version on PubMed Central for supplementary material.

Acknowledgements

We thank P.R. Rapp, J. Long, S.M. Raver and V. Stuphorn for critical discussions and reading of the manuscript; H.M.V. Manzur and B. Brock for technical support. This research is funded by the Intramural Research Program of the National Institute on Aging (NIH, USA) and by NARSAD Young Investigator Award to S.L., NIH P01 AG09973 to M.G. and NIH F31 AG045039 to J.D.M.

References

1. Boucher L, Palmeri TJ, Logan GD, Schall JD. Inhibitory control in mind and brain: An interactive race model of countermanding Saccades. *Psychol. Rev.* 2007; 114:376–397. [PubMed: 17500631]
2. Aron AR. From reactive to proactive and selective control: developing a richer model for stopping inappropriate responses. *Biol. Psychiatry.* 2011; 69:e55–68. [PubMed: 20932513]
3. Schall JD, Godlove DC. Current advances and pressing problems in studies of stopping. *Curr. Opin. Neurobiol.* 2012; 22:1012–1021. [PubMed: 22749788]
4. Stuphorn V. Neural mechanisms of response inhibition. *Curr. Opin. Behav. Sci.* 2014 doi:10.1016/j.cobeha.2014.10.009.
5. Aron AR, et al. Converging Evidence for a Fronto-Basal-Ganglia Network for Inhibitory Control of Action and Cognition. *J. Neurosci.* 2007; 27:11860–11864. [PubMed: 17978025]
6. Logan GD, Cowan WB. On the ability to inhibit thought and action: A theory of an act of control. *Psychol. Rev.* 1984; 91:295–327.
7. Mayse JD, Nelson GM, Park P, Gallagher M, Lin S-C. Proactive and reactive inhibitory control in rats. *Front. Neurosci.* 2014; 8:104. [PubMed: 24847204]
8. Gauggel S, Rieger M, Feghoff T-A. Inhibition of ongoing responses in patients with Parkinson's disease. *J. Neurol. Neurosurg. Psychiatry.* 2004; 75:539–544. [PubMed: 15026491]
9. Mirabella G, et al. Deep Brain Stimulation of Subthalamic Nuclei Affects Arm Response Inhibition In Parkinson's Patients. *Cereb. Cortex (New York, N.Y. 1991).* 2011 doi:10.1093/cercor/bhr187.
10. McAlonan GM, et al. Age-related grey matter volume correlates of response inhibition and shifting in attention-deficit hyperactivity disorder. *Br. J. Psychiatry J. Ment. Sci.* 2009; 194:123–129.
11. Andrés P, Guerrini C, Phillips LH, Perfect TJ. Differential effects of aging on executive and automatic inhibition. *Dev. Neuropsychol.* 2008; 33:101–123. [PubMed: 18443972]
12. Coxon JP, Impe A, Van, Wenderoth N, Swinnen SP. Aging and Inhibitory Control of Action: Cortico-Subthalamic Connection Strength Predicts Stopping Performance. *J. Neurosci.* 2012; 32:8401–8412. [PubMed: 22699920]
13. Hu S, Chao HH-A, Zhang S, Ide JS, Li C-SR. Changes in cerebral morphometry and amplitude of low-frequency fluctuations of BOLD signals during healthy aging: correlation with inhibitory control. *Brain Struct. Funct.* 2013 doi:10.1007/s00429-013-0548-0.
14. Eagle DM, et al. Stop-signal reaction-time task performance: role of prefrontal cortex and subthalamic nucleus. *Cereb. Cortex (New York, N.Y. 1991).* 2008; 18:178–188.
15. Baunez C, et al. Effects of STN lesions on simple vs choice reaction time tasks in the rat: preserved motor readiness, but impaired response selection. *Eur. J. Neurosci.* 2001; 13:1609–1616. [PubMed: 11328354]

16. Duann JR, Ide JS, Luo X, Li CS. Functional connectivity delineates distinct roles of the inferior frontal cortex and presupplementary motor area in stop signal inhibition. *J Neurosci.* 2009; 29:10171–10179. [PubMed: 19675251]
17. Li CS, Yan P, Sinha R, Lee TW. Subcortical processes of motor response inhibition during a stop signal task. *Neuroimage.* 2008; 41:1352–1363. [PubMed: 18485743]
18. Schmidt R, Leventhal DK, Mallet N, Chen F, Berke JD. Canceling actions involves a race between basal ganglia pathways. *Nat. Neurosci.* 2013; 16:1118–24. [PubMed: 23852117]
19. Freund TF, Gulyás AI. GABAergic interneurons containing calbindin D28K or somatostatin are major targets of GABAergic basal forebrain afferents in the rat neocortex. *J Comp Neurol.* 1991; 314:187–199. [PubMed: 1686776]
20. Gritti I, Mainville L, Mancia M, Jones BE. GABAergic and other noncholinergic basal forebrain neurons, together with cholinergic neurons, project to the mesocortex and isocortex in the rat. *J Comp Neurol.* 1997; 383:163–177. [PubMed: 9182846]
21. Richardson RT, DeLong MR. Context-dependent responses of primate nucleus basalis neurons in a go/no-go task. *J. Neurosci.* 1990; 10:2528–40. [PubMed: 2388078]
22. Lin S-C, Nicolelis MAL. Neuronal ensemble bursting in the basal forebrain encodes salience irrespective of valence. *Neuron.* 2008; 59:138–49. [PubMed: 18614035]
23. Avila I, Lin S-C. Distinct neuronal populations in the basal forebrain encode motivational salience and movement. *Front. Behav. Neurosci.* 2014; 8:1–12. [PubMed: 24478648]
24. Avila I, Lin S-C. Motivational salience signal in the basal forebrain is coupled with faster and more precise decision speed. *PLoS Biol.* 2014; 12:e1001811. [PubMed: 24642480]
25. Lin S-C, Gervasoni D, Nicolelis MAL. Fast modulation of prefrontal cortex activity by basal forebrain noncholinergic neuronal ensembles. *J. Neurophysiol.* 2006; 96:3209–3219. [PubMed: 16928796]
26. Nguyen DP, Lin S-C. A frontal cortex event-related potential driven by the basal forebrain. *Elife.* 2014; 3:e02148–e02148. [PubMed: 24714497]
27. Stuphorn V, Taylor TL, Schall JD. Performance monitoring by the supplementary eye field. *Nature.* 2000; 408:857–60. [PubMed: 11130724]
28. Matsumoto M, Hikosaka O. Two types of dopamine neuron distinctly convey positive and negative motivational signals. *Nature.* 2009; 459:837–841. [PubMed: 19448610]
29. Bromberg-Martin ES, Matsumoto M, Hikosaka O. Distinct tonic and phasic anticipatory activity in lateral habenula and dopamine neurons. *Neuron.* 2010; 67:144–55. [PubMed: 20624598]
30. Butovas S, Schwarz C. Spatiotemporal effects of microstimulation in rat neocortex: a parametric study using multielectrode recordings. *J. Neurophysiol.* 2003; 90:3024–39. [PubMed: 12878710]
31. Butovas S, Hormuzdi SG, Monyer H, Schwarz C. Effects of electrically coupled inhibitory networks on local neuronal responses to intracortical microstimulation. *J. Neurophysiol.* 2006; 96:1227–36. [PubMed: 16837655]
32. Long JD, Carmena JM. Dynamic changes of rodent somatosensory barrel cortex are correlated with learning a novel conditioned stimulus. *J. Neurophysiol.* 2013; 109:2585–95. [PubMed: 23468389]
33. Watanabe K, Lauwereyns J, Hikosaka O. Neural correlates of rewarded and unrewarded eye movements in the primate caudate nucleus. *J. Neurosci.* 2003; 23:10052–10057. [PubMed: 14602819]
34. Jin X, Tecuapetla F, Costa RM. Basal ganglia subcircuits distinctively encode the parsing and concatenation of action sequences. *Nat. Neurosci.* 2014; 2014
35. Jahfari S, et al. How Preparation Changes the Need for Top-Down Control of the Basal Ganglia When Inhibiting Premature Actions. *J. Neurosci.* 2012; 32:10870–10878. [PubMed: 22875921]
36. Jin X, Costa R. Start/stop signals emerge in nigrostriatal circuits during sequence learning. *Nature.* 2010; 466:457–462. [PubMed: 20651684]

Method-Only References

37. Paxinos, G.; Watson, C. The rat brain in stereotaxic coordinates. Acad. Press.; San Diego: 2007. Academic Press
38. Wiest MC, Bentley N, Nicolelis M. a L. Heterogeneous integration of bilateral whisker signals by neurons in primary somatosensory cortex of awake rats. J. Neurophysiol. 2005; 93:2966–73. [PubMed: 15563555]

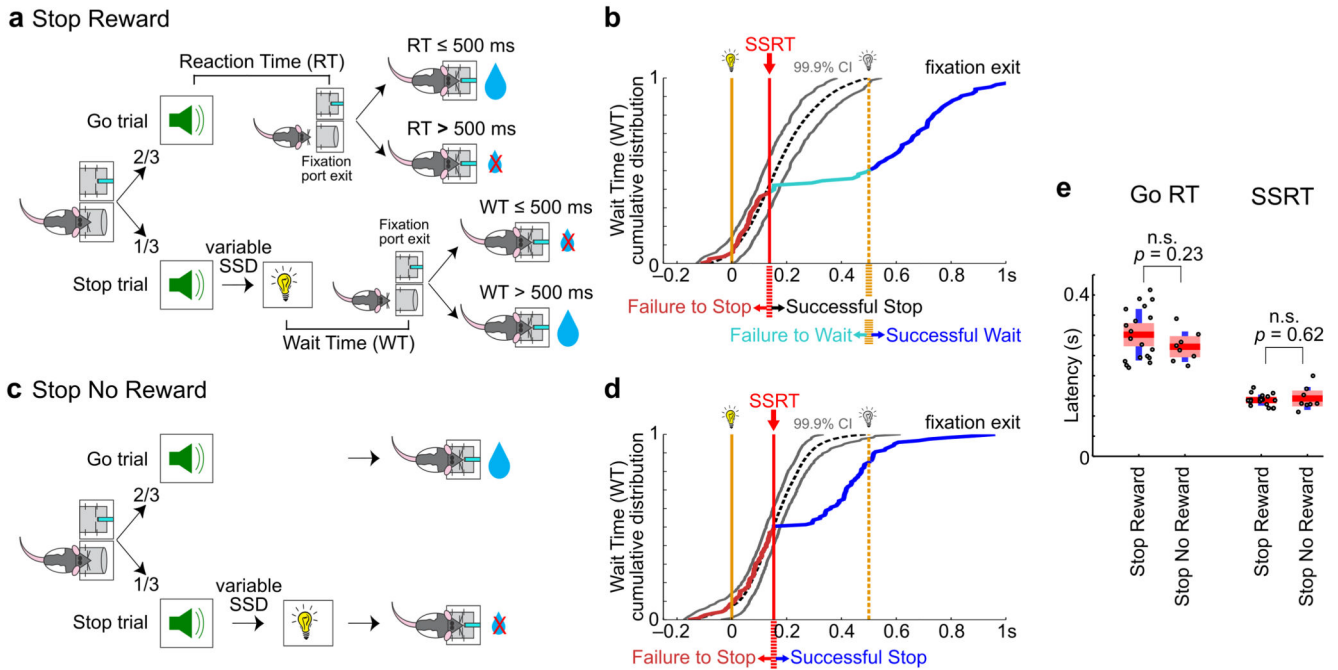


Figure 1. Similar rapid behavioral stopping regardless of whether successful stopping is rewarded

(a, c) Schematic of the Stop Reward Task **(a)** and Stop No Reward Task **(c)**. In the Stop Reward Task, each trial was initiated by the rat entering the fixation port, followed by the same go sound in all trials signaling reward in the adjacent port if reaction time (RT) was 500ms. On stop trials, the go sound was followed by a stop light after a variable stop signal delay (SSD). Rats were rewarded on these trials if they canceled the go response and the wait time (WT, response latency relative to stop signal onset) was > 500 ms. The Stop No Reward Task had the same sequence of events, except that stop trials were never rewarded. **(b, d)** Example sessions from the Stop Reward Task **(b)** and the Stop No Reward Task **(d)** showing cumulative distributions of WT. Yellow dashed lines indicate the offset of the stop signal and the end of the waiting period. SSRT was determined by comparing the cumulative WT distribution in stop trials with latency-matched go trials (gray lines indicate 99.9% confidence interval) (see Methods for details). Fixation port exits before SSRT were classified as failure-to-stop trials while those after SSRT were classified as successful stop trials. Successful stop trials in the Stop Reward Task were further classified into failure-to-wait and successful wait trials depending on whether rats waited long enough to receive reward. **(e)** Go RT and SSRT were not significantly different between the two SST variants. Individual animals (points) are plotted along with group mean (red), ± 1.96 s.e.m. (red shaded area) and ± 1 s.d. (blue) (Stop Reward: $n = 19$ rats, 543 sessions; Stop No Reward: $n = 8$ rats, 466 sessions).

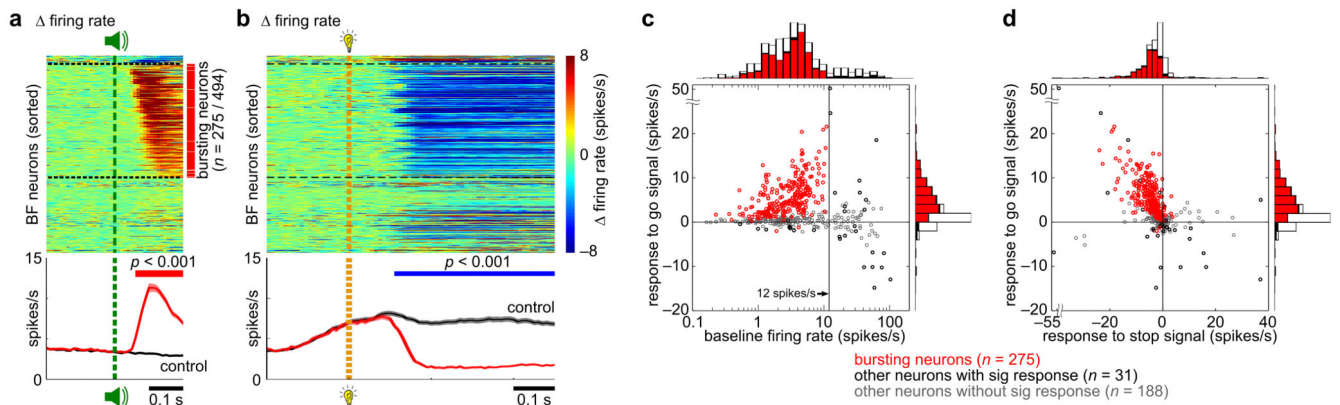


Figure 2. BF neurons with bursting responses to the go signal were inhibited nearly completely by the stop signal, irrespective of whether successful stopping was rewarded

(a) (top) Responses of individual BF neurons collapsed across both SST variants ($n=494$) to the go signal, shown as the difference between go trials and foreperiod-matched controls. Individual BF neurons were sorted by the latency of the first significant response within 200ms of go signal onset. Black dotted lines separate neurons with significant inhibitory responses ($n=21$), excitatory responses ($n=285$), and no response ($n=188$) to the go signal. Bursting neurons were identified as BF neurons with an excitatory response within 200ms of go signal onset and a baseline firing rate less than 12 Hz (275/285) (red vertical bar). (bottom) Population PSTH (mean \pm s.e.m.) for bursting neurons in go trials and foreperiod-matched controls, with significant excitation indicated by the red horizontal bar (Bonferroni-corrected paired t-test for each 10ms bin). (b) Responses of the same individual BF neurons to the stop signal, shown as the difference between stop trials and latency-matched go trial controls. The sorting order of BF neurons in the top panel is the same as in (a). The blue horizontal bar in the bottom panel indicates significant inhibition. Conventions are the same as in (a). (c) Scatter plot of the average firing rate in the [0.05, 0.2]s window after the go signal vs. baseline firing rate for individual BF neurons, and corresponding marginal distributions. (d) Scatter plot of the average firing rates in the [0.05, 0.2]s window after the go signal vs. in the [0.1, 0.5]s window after the stop signal for individual BF neurons, and corresponding marginal distributions. Bursting neurons are indicated in red, other neurons with significant responses to the go signal are indicated in black, and neurons with no significant responses are indicated in gray.

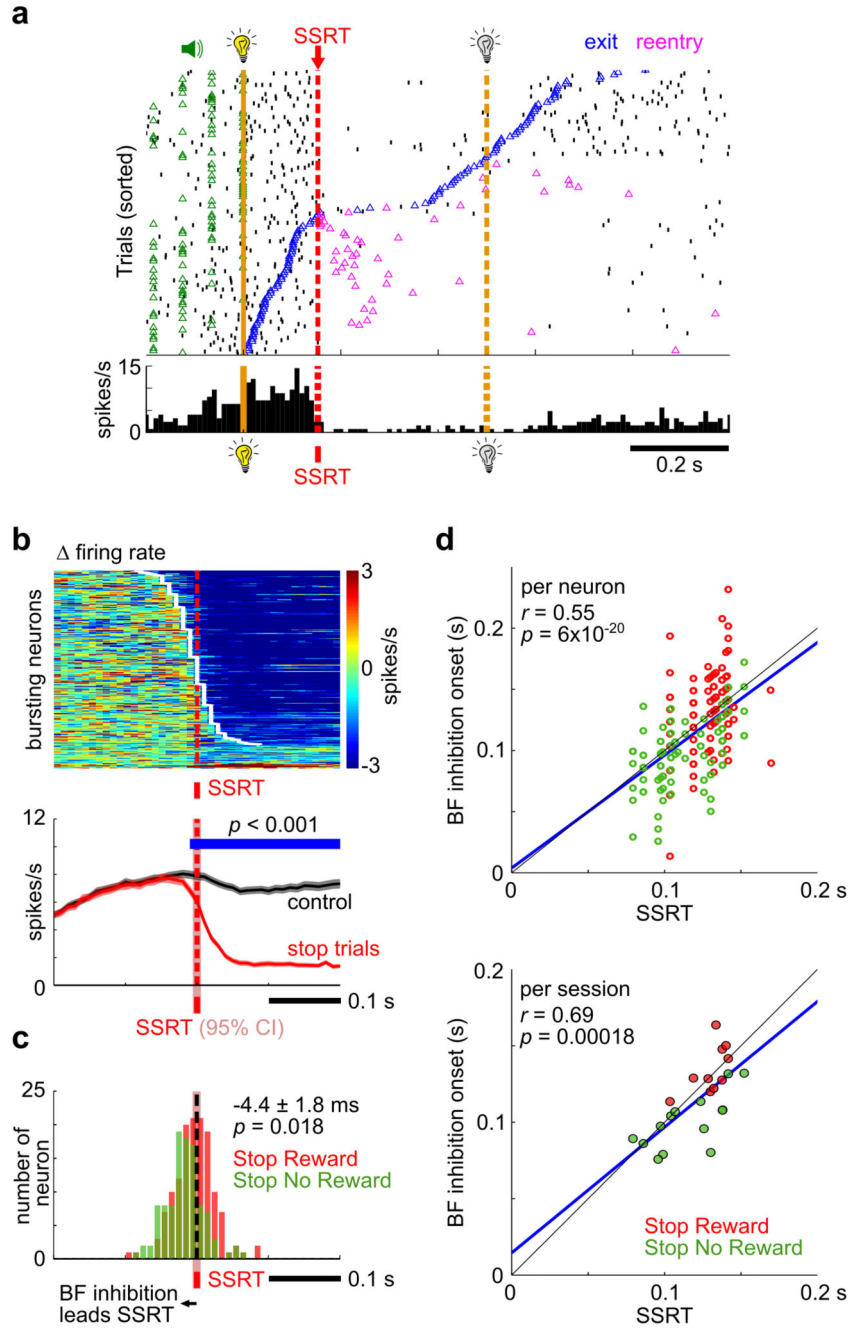


Figure 3. The latency of BF neuronal inhibition was coupled with and slightly preceded SSRT, irrespective of whether successful stopping was rewarded
(a) Raster plot of an example BF bursting neuron in the Stop Reward Task. Stop trials were aligned to stop signal onset and sorted by fixation port exit time. Near complete neuronal inhibition began around SSRT. **(b)** Response of BF bursting neurons to the stop signal, aligned at the estimated SSRT within each session. Top, BF bursting neurons ($n=275$ neurons) were sorted based on the latency of neuronal inhibition (white line). Bottom, the population PSTH shows that the onset of BF inhibition preceded SSRT by at least 10ms. **(c)**

Histogram of neuronal inhibition latency for BF bursting neurons in the Stop Reward Task ($n=138$) and Stop No Reward Task ($n=104$) relative to SSRT. The red shaded areas around SSRT in **(b)** and **(c)** reflect the 95% confidence interval of the mean SSRT estimate ($n=37$ sessions) (see Methods for details). **(d)** Strong correlation between SSRT and the onset of neuronal inhibition for individual BF bursting neurons (top) and for sessions with at least 4 BF bursting neurons (bottom, $n=24$ sessions). The blue line is the linear regression fit.

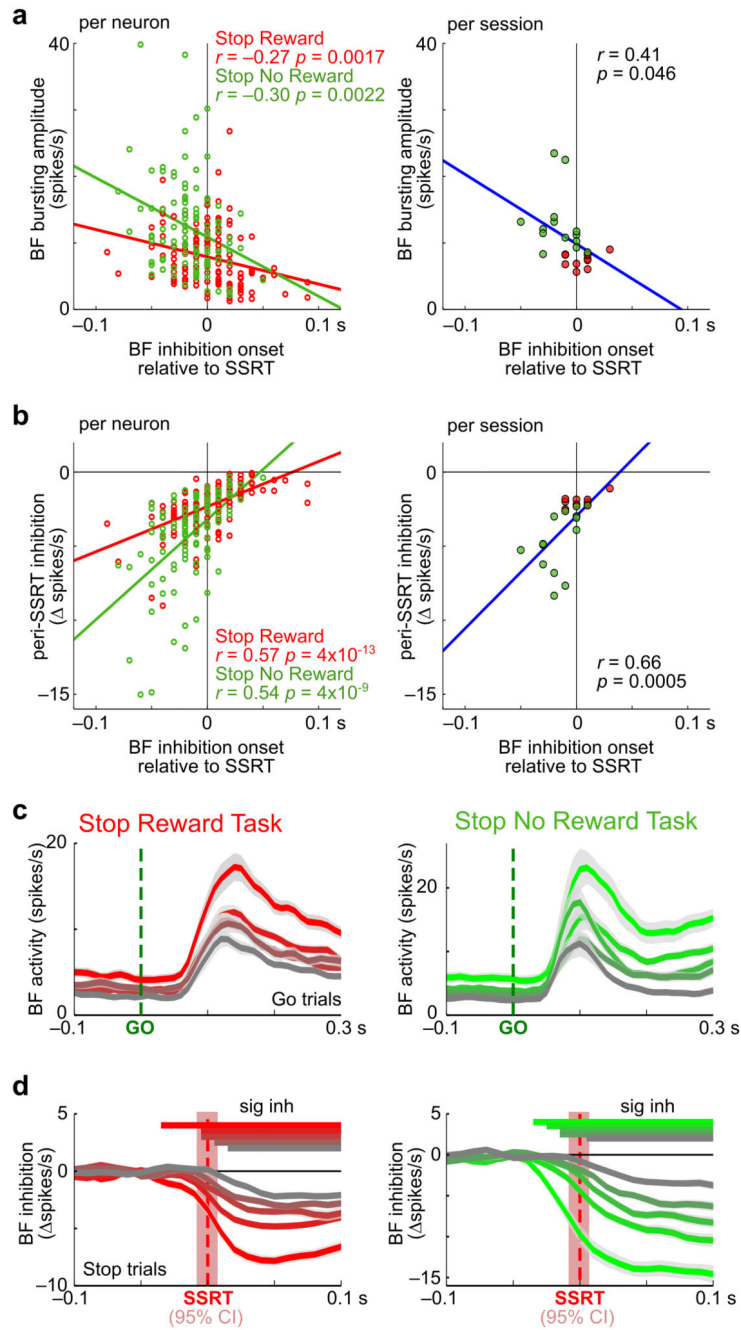


Figure 4. Strongly bursting BF neurons were inhibited more by the stop signal and with earlier inhibition latencies before SSRT

(a) Significant correlation between BF bursting amplitude to the go signal and neuronal inhibition latency relative to SSRT in both SST variants. Results were plotted separately for individual BF bursting neurons (left, $n=138$, 104) and for sessions with at least 4 BF bursting neurons (right; $n=24$). **(b)** Significant correlation between peri-SSRT inhibition by the stop signal and neuronal inhibition latency relative to SSRT in both SST variants. **(c-d)** BF bursting neurons were sorted into five quintiles based on their peri-SSRT inhibition

amplitude, separately for the two SST variants. The 1st quintile is shown in red/green, while the 5th quintile in gray. Average responses of each quintile (mean \pm s.e.m.) to the go signal in go trials (**c**) and peri-SSRT inhibition in all stop trials (**d**). Bins showing significant inhibition around SSRT are labeled by horizontal lines for each quintile. BF neurons that were inhibited earlier relative to SSRT were inhibited more by the stop signal and excited more by the go signal. The red shaded areas indicate the 95% CI of SSRT estimate ($n=17$, 20 sessions).

Author Manuscript

Author Manuscript

Author Manuscript

Author Manuscript

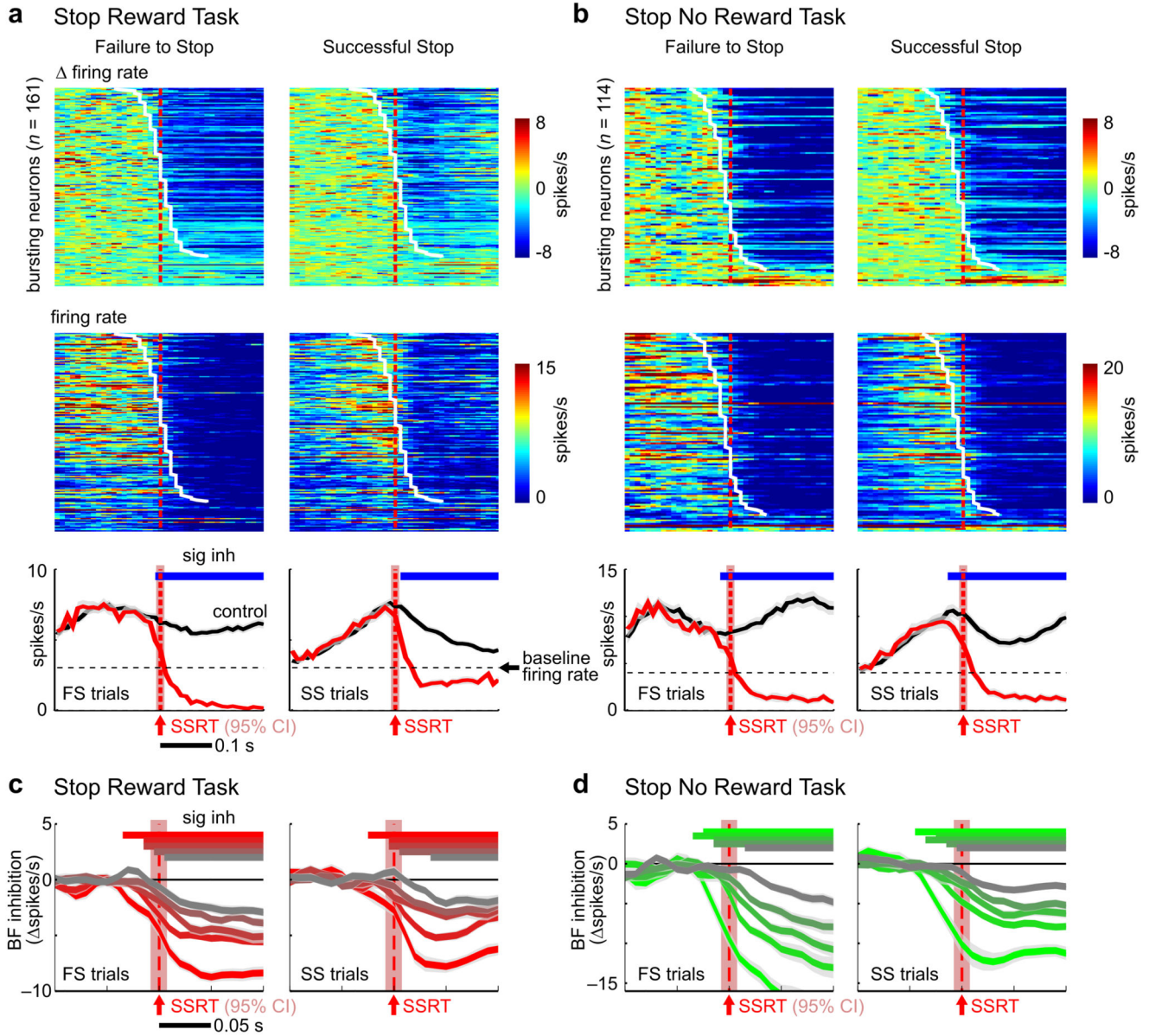


Figure 5. BF neuronal inhibition was similarly engaged regardless of whether stopping was successful

(a-b) Responses of BF bursting neurons to the stop signal aligned at SSRT, plotted separately for failure-to-stop (left) and successful stop trials (right), and separately for the Stop Reward (a) and Stop No Reward tasks (b). Top row, rate changes in stop trials compared to latency-matched controls. BF bursting neurons were sorted by inhibition latency (white line). Middle row, firing rates in stop trials. Bottom row, population PSTHs aligned to SSRT show that BF neurons were inhibited below baseline firing rates (black dashed line). BF neuronal inhibition was present and time-locked to SSRT in both failure-to-stop and successful stop trials in both SST variants. (c-d) Peri-SSRT inhibition of the five quintiles of BF bursting neurons (mean \pm s.e.m.), as defined in Fig.4c-d, in failure-to-stop and successful stop trials. Note that the top three quintiles of BF bursting neurons in

successful stop trials are still inhibited 10ms before SSRT. The red shaded areas indicate the 95% CI of SSRT estimate ($n=17$, 20 sessions).

Author Manuscript

Author Manuscript

Author Manuscript

Author Manuscript

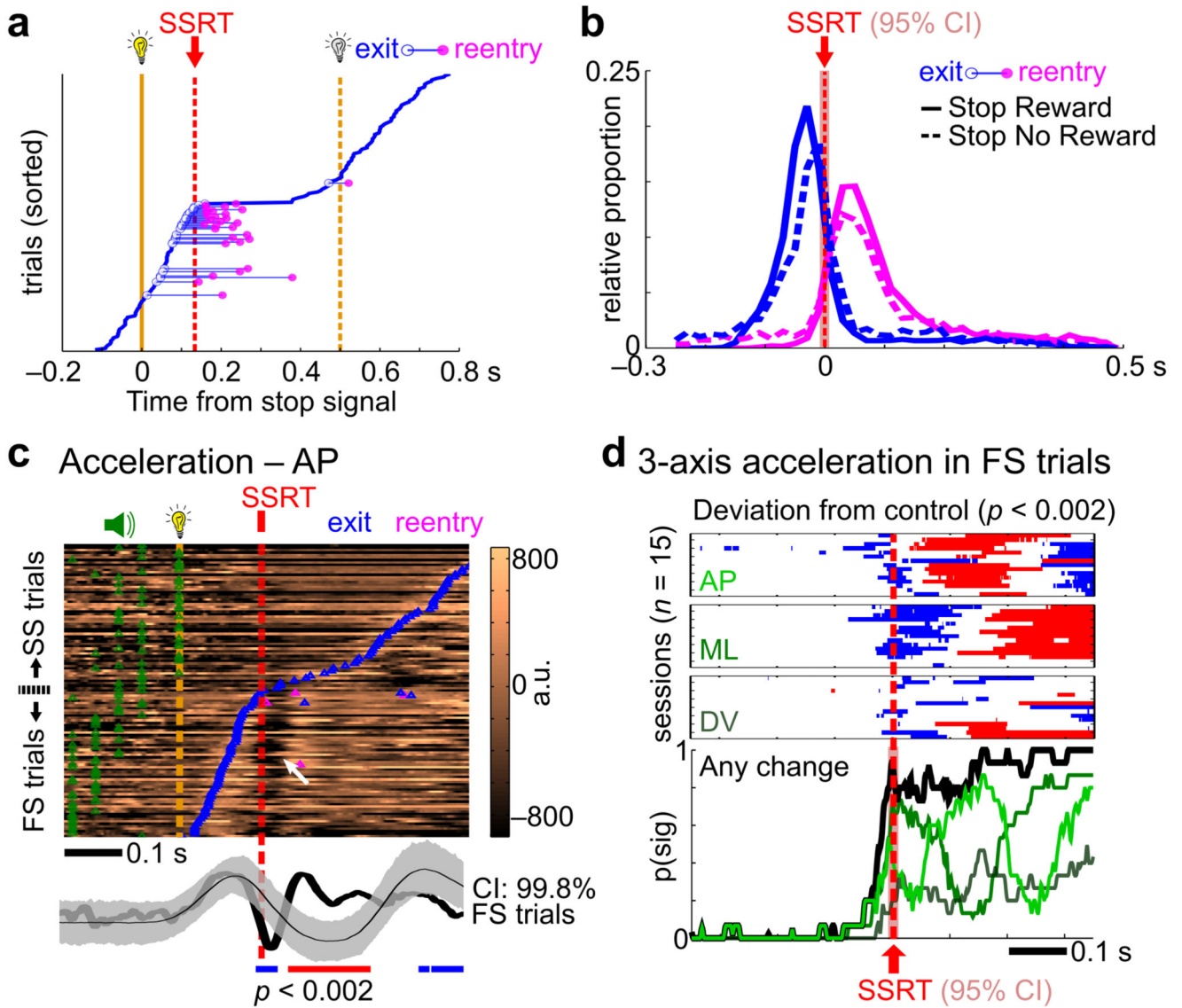


Figure 6. BF neuronal inhibition in failure-to-stop trials was associated with corrective fixation port reentries and reversal of head movements at SSRT
(a) An example session from the Stop Reward Task showing frequent fixation port reentry events in failure-to-stop trials, especially when rats exited the fixation port just before SSRT.
(b) The distribution of fixation port exit and reentry events in all reentry trials. For both SST variants, fixation port exit and reentry events were most common just before and after SSRT, respectively.
(c) Head-mounted accelerometer signal from an example session in the Stop No Reward Task. The top panel shows color-coded accelerometer signals in single trials, with prominent reversal of movement acceleration in failure-to-stop trials occurring at SSRT (white arrow). The bottom panel shows the averages of accelerometer signals from failure-to-stop trials (black) and matching go trial controls (gray areas indicate the CI, see Methods for details). Horizontal bars indicate significant ($p < 0.002$) decreases (blue) or increases (red) in accelerometer signals in failure-to-stop trials.
(d) The time course of when

accelerometer signals in failure-to-stop trials were significantly different from matching go trial controls. Significant bins were plotted separately for the 3 accelerometer axes in 15 sessions, with the aggregate probabilities shown below. Significant differences in accelerometer signals in failure-to-stop trials began at SSRT. The red shaded areas indicate the 95% CI of SSRT estimate ($n=15$ sessions).

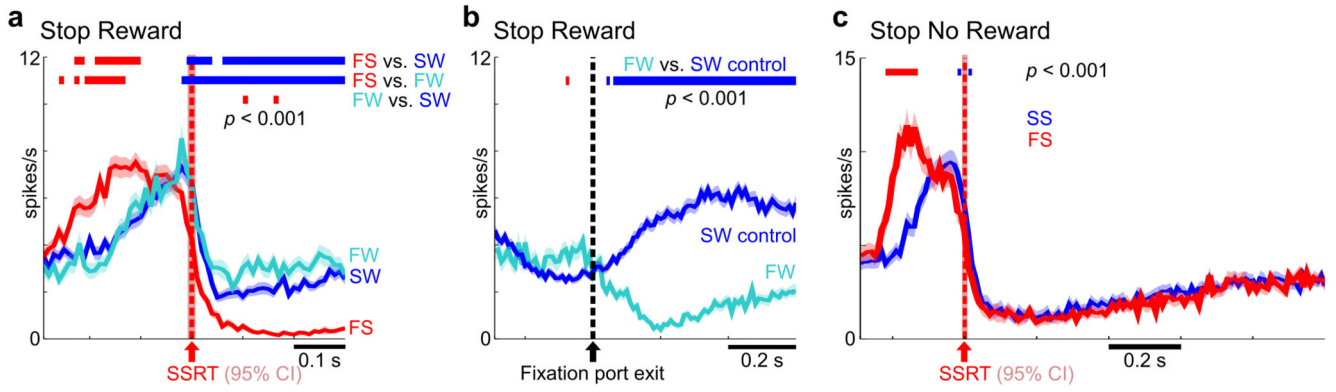


Figure 7. Post-SSRT BF activity tracked reward expectancy and behavioral performance
(a) Population PSTHs (mean \pm s.e.m.) of BF bursting neurons in the Stop Reward Task for the three trial types. Horizontal bars indicate significant ($p < 0.001$) decreases (blue) or increases (red) in activity. Activity in failure-to-stop trials was significantly lower than the other two trial types after SSRT. Activity in failure-to-wait trials was significantly higher than successful wait trials during the waiting period after SSRT. Significant differences in activity before SSRT disappear when SSDs are properly matched (Fig. 5a). **(b)** Population PSTHs of BF bursting neurons in the Stop Reward Task for failure-to-wait and successful wait trials, aligned at fixation port exit of failure-to-wait trials (see Methods for details). Activity in failure-to-wait trials was significantly higher than latency-matched successful wait trials and peaked right before fixation port exit. After fixation port exit, activity in failure-to-wait trials immediately decreased relative to successful wait trials. **(c)** Population PSTHs of BF bursting neurons in the Stop No Reward Task for the two trial types. There was no significant difference in neuronal activity between failure-to-stop and successful stop trials after SSRT. Again, significant differences in activity before SSRT disappear when SSDs are properly matched (Fig. 5b). ($n = 161$ neurons for Stop Reward Task, $n = 114$ for Stop No Reward Task). The red shaded areas indicate the 95% CI of SSRT estimate ($n = 17, 20$ sessions).

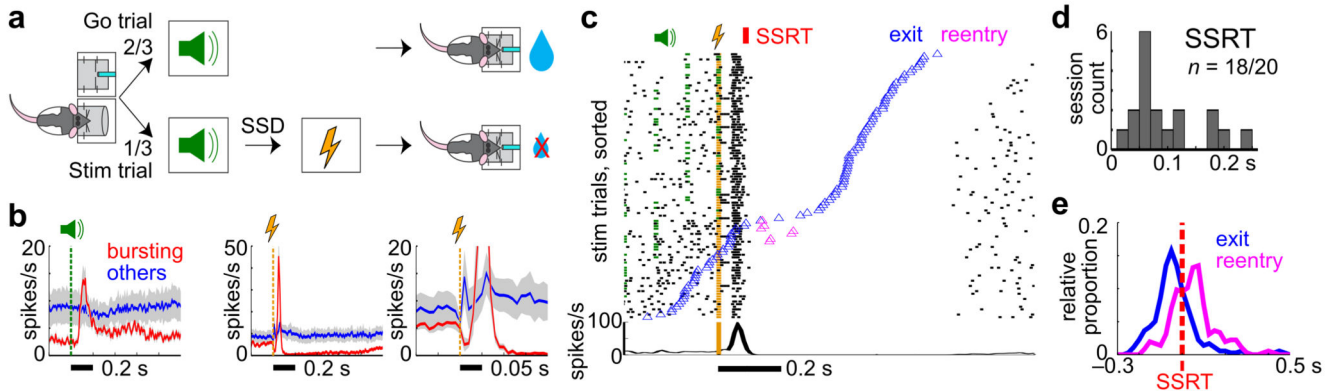


Figure 8. Induced BF inhibition in place of the stop signal reproduced behavioral stopping and reentry behavior in rats naive to SST training

(a) Schematic of the electrical stimulation experiment, which was the same as the Stop No Reward Task except that the stop signal was replaced by brief BF electrical stimulation. (b) Response of bursting ($n=21$) and other ($n=23$) BF neurons to the go sound (left panel) and brief BF electrical stimulation (middle and right panels show different time scales, 11 sessions from 4 rats). BF bursting neurons, but not other neurons, demonstrated near complete inhibition in response to BF electrical stimulation after a brief rebound excitation. (c) An example BF bursting neuron in stimulated trials. The onset of sustained BF inhibition coincides with estimated SSRT. Reentry was observed in trials where rats exited the fixation port right before SSRT, similar to the reentry behavior in the SST (Fig. 6a). (d) Distribution of estimated SSRT from 18/20 sessions (7 rats) showing significant slowing of fixation port exit in response to BF electrical stimulation. (e) The distribution of fixation port exit and reentry events in all reentry trials in the stimulation experiment. Fixation port exit and reentry events were most common just before and after SSRT, respectively.